

# Doppler imaging of the double-lined active binary V824 Ara

L. Kriskovics<sup>1,\*</sup>, K. Vida<sup>1</sup>, Zs. Kővári<sup>1</sup>, D. Garcia-Alvarez<sup>2,3,4</sup>, and K. Oláh<sup>1</sup>

<sup>1</sup>Research Centre for Astronomy and Earth Sciences, Hungarian Academy of Sciences

<sup>2</sup>Instituto de Astrofísica de Canarias, E-38205 La Laguna, Tenerife, Spain

<sup>3</sup>Dpto. de Astrofísica, Universidad de La Laguna, 38206 La Laguna, Tenerife, Spain

<sup>4</sup>Grantecan CALP, 38712 Breña Baja, La Palma, Spain

Received 30 May 2005, accepted 11 Nov 2005

Published online later

**Key words** stars: activity – stars: Doppler imaging – stars: late-type – stars: starspots – stars: individual: V824 Ara (HD 155555)

We introduce an iterative spectral disentangling technique combined with Doppler imaging in order to recover surface temperature maps for both components of double-lined active binary systems. Our method provides an opportunity to separate spectra of the active components while minimizing the unwanted disturbances on the given line profile from the other component. The efficiency of the method is demonstrated on real data of the double-lined RS CVn-type binary V824 Ara. The resulting Doppler images reveal cool spots on the polar regions as well as low-latitude features on both of the stars. Moreover, both components have hot spots, that are facing each other. This may indicate interconnection between the stellar magnetic fields.

© 2013 WILEY-VCH Verlag GmbH & Co. KGaA, Weinheim

## 1 Introduction

Doppler imaging of components in a double-lined active binary is a challenging task. Disentangling the spectra of the components is essential, however, fairly difficult, for the very reason of the line profile distortions due to starspots on both components. Still, there are different strategies to follow. The simplest approach to handle this issue is omitting the blended phases from the inversion process (Strassmeier & Rice 2000). But this way sufficiently good phase coverage can easily be lost, together with all the information on the blended phases, where spectra from the two components overlap.

Another possibility is to apply simultaneous Doppler imaging for the two components, however, the number of the inversion parameters becomes nearly double, consequently, the reliability of the results is reduced. But again, in blended phases the separation of distortions originating from the spots on different components is still unsolved (as an attempt, in blended phases usually homogeneous surface is assumed for the secondary component). Among the very few examples in the literature, see e.g., the application of a two-line Doppler imaging code for  $\sigma^2$  CrB by Strassmeier & Rice (2003), and the Doppler tomography of ER Vul and TY Pyx in Piskunov (2001). Among double-lined active binaries V824 Ara (HD 155555) is the most thoroughly studied system. In the paper by Hatzes & Kürster (1999) rotationally broadened synthetic spectra were fitted to the observations and the blended line profiles were subtracted before applying Doppler imaging. Their maps showed polar active

HJD	phase	dd-mm-yyyy	$\Delta\lambda$ [Å]	S/N
2450536.611	0.55	19-09-2002	6403–6447	121
2450537.645	0.16	20-09-2002	6403–6447	113
2450538.501	0.67	20-09-2002	6403–6447	111
2450538.612	0.74	21-09-2002	6403–6447	124
2450539.479	0.26	21-09-2002	6403–6447	109
2450539.580	0.32	21-09-2002	6403–6447	104
2450539.640	0.35	21-09-2002	6403–6447	101
2450540.477	0.85	21-09-2002	6403–6447	110
2450540.531	0.88	22-09-2002	6403–6447	106
2450540.614	0.93	22-09-2002	6403–6447	117

**Table 1** The table gives the HJDs of the observations, the corresponding phases calculated using Eq. 1 from Sect. 3, the observing dates, the wavelength regions ( $\Delta\lambda$ ) and the measured signal-to-noise (S/N) ratios.

regions on both components, and several low latitudinal features. In Strassmeier & Rice (2000) the blended phases were simply excluded from the inversion process. Their results revealed also polar spots, but at lower latitudes spot distribution was different compared to the ones of Hatzes & Kürster (1999). Zeeman–Doppler imaging was applied for V824 Ara by Dunstone et al. (2008) where Stokes  $I$  maps showed polar features as well.

In this paper we introduce an iterative spectral disentangling technique combined with Doppler imaging in order to recover surface temperature maps for both components of V824 Ara. In our new approach profiles in the blended phases are treated to preserve information on the surface spot distribution.

\* Corresponding author: e-mail: kriskovics.levente@csfk.mta.hu

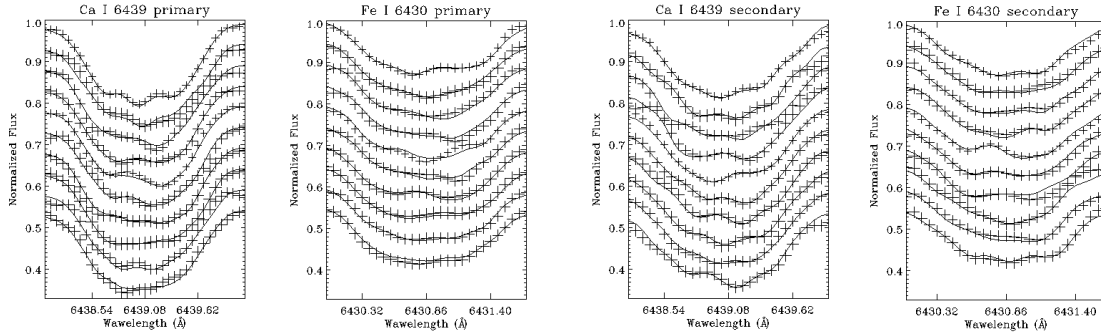


**Fig. 1** Line profile fits (solid lines) to the observations (crosses). From left to right: Ca I 6439 Å (1st panel) and Fe I 6430 Å profiles (2nd panel) of the primary component, Ca I 6439 Å (3rd panel) and Fe I 6430 Å profiles (4th panel) of the secondary component. The size of the crosses indicates the S/N.

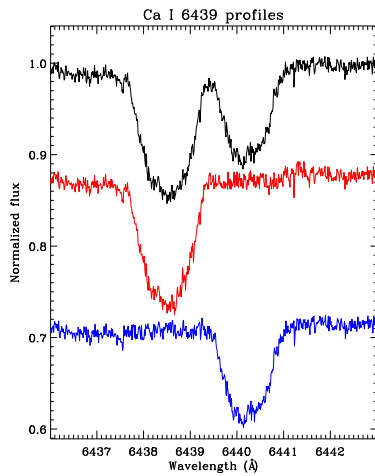


**Fig. 2** An example of disentangled spectra at phase  $\phi=0.411$ : the original blended spectra from the Ca I 6439 Å region (top), and the contributions of the primary (middle) and the secondary (bottom) components. Note that the downward shifts of the contribution spectra are optional.

## 2 The method

In case of a double-lined binary with two spotted components, the separation of the profiles is troublesome, but essential. First we set the relative continuum contributions of the two components (which are 0.7 and 0.3 for the primary and the secondary components of V824 Ara, respectively, see Strassmeier & Rice 2000). Then, we apply an iterative method, which ensures an effective subtraction even at blended phases where the spectral lines from the primary and the secondary stars heavily overlap. Our method, step by step:

- an initial line profile of the secondary component is calculated by synthesizing an undisturbed line profile (i.e., assuming a homogeneous surface);
- the initial profile is subtracted from the composite spectrum providing a preliminary line profile of the primary component;

Parameter	Primary	Secondary
$T_{\text{eff}}$	$5400 \pm 100$ K	$5040 \pm 150$ K
$\log g$	$4.0 \pm 0.5$	$4.5 \pm 0.5$
$v \sin i$	$36.9 \pm 1.0$ km/s	$33.5 \pm 1.0$ km/s
Inclination $i$	$55^\circ \pm 5$	$55^\circ \pm 5$
Microturbulence $\zeta_{Ca}$	1.5 km/s	1.5 km/s
Microturbulence $\zeta_{Fe}$	2.0 km/s	1.5 km/s

**Table 2** Basic astrophysical parameters for V824 Ara adopted for Doppler reconstructions from Strassmeier & Rice (2000).

- the set of preliminary profiles are used to perform Doppler imaging (DI) of the primary component;
- from the resulting image line profiles of the primary component are calculated with using the forward version of our DI code;
- profiles from the forward DI process are subtracted from the original spectra to get profiles of the secondary component;
- resulting profiles are used to perform Doppler imaging for the secondary component;
- Doppler maps of the secondary star are used as input to calculate distorted line profiles of the secondary with the forward DI code;
- these profiles of the secondary are subtracted from the original spectra;
- resulting spectra are used to derive Doppler maps for the primary component.

The above steps are repeated iteratively until the Doppler images are converged.

## 3 Doppler imaging of V824 Ara

### 3.1 Spectroscopic data

10 spectra were taken between 19 and 22 Sept 2002 with the Coudé-Echelle Spectrometer and with the Loral  $2688 \times 512$   $15\mu$  CCD mounted on the ESO 3.6 m telescope (3P6) in

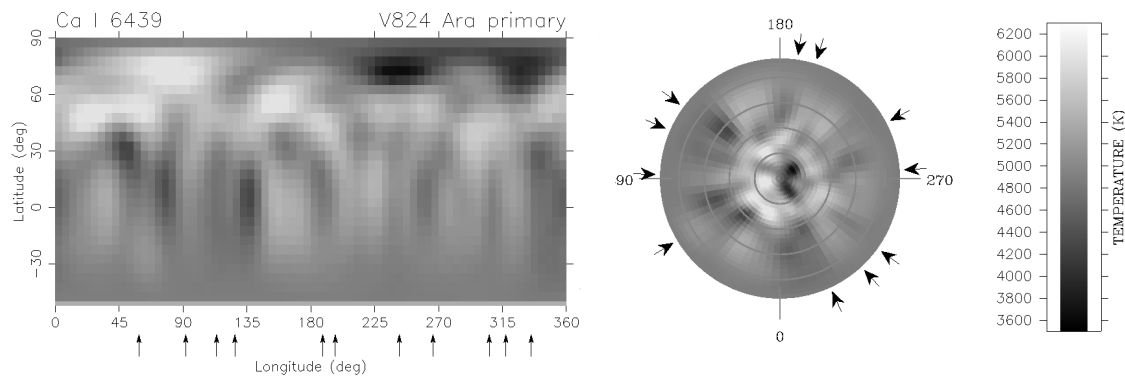


**Fig. 3** Resulting Doppler reconstruction of the primary component of V824 Ara for the Ca I 6439 Å line. The surface temperature map is plotted in pseudo-Mercator projection (left) and in pole-on view (right). Arrows mark the phases of the observations.

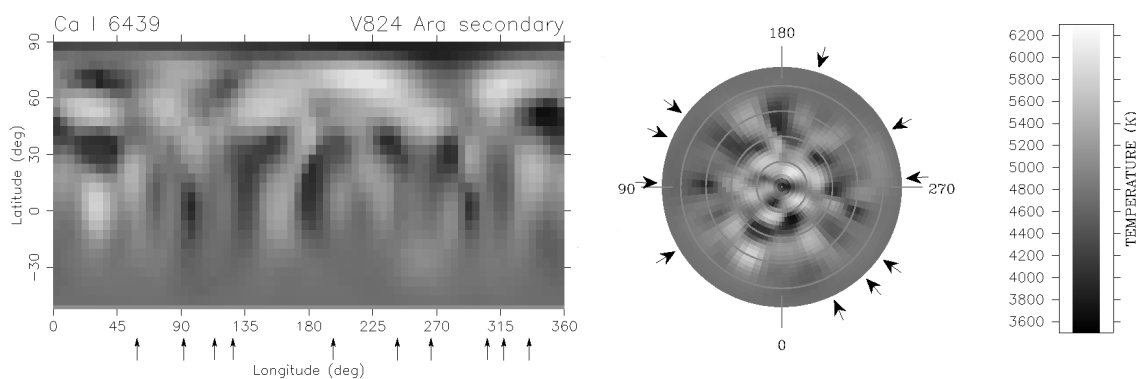


**Fig. 4** Resulting Doppler reconstruction of the secondary component of V824 Ara for the Ca I 6439 Å line. The surface temperature map is plotted in pseudo-Mercator projection (left) and in pole-on view (right). Arrows mark the phases of the observations.

La Silla, Chile. The observations were carried out in single-order mode covering the 6400–6450 Å range with the exposure time of 900 s, typically providing signal-to-noise ratios of 100–125 at peak resolution  $R = 65,000$ . The gathered data cover one orbital cycle with suitable phase sampling to perform Doppler imaging. Table 1 summarizes the observing log. Phases are calculated using the following equation (Strassmeier & Rice 2000):

$$\text{HJD} = 2,446,998.4102 + 1.6816 \times E. \quad (1)$$

Data reduction was carried out using the standard NOAO/IRAF<sup>1</sup> routines.

### 3.2 Astrophysical parameters

Basic input parameters for Doppler imaging were adopted from Strassmeier & Rice (2000). However, the inclination  $i$  and projected equatorial velocity  $v \sin i$  values are fine-tuned with a grid search method based on finding the best fit  $\chi^2$  from Doppler reconstructions over a reasonable part of the parameter plane (for the method see Unruh 1996).

<sup>1</sup> IRAF is distributed by the National Optical Astronomy Observatory, which is operated by the Association of Universities for Research in Astronomy (AURA) under cooperative agreement with the National Science Foundation.

Accordingly, for this study we used  $v \sin i = 36.9$  km/s for the primary, and  $v \sin i = 33.5$  km/s for the secondary component. The former value is slightly higher, while the latter is lower compared to the ones in Strassmeier & Rice (2000). The errors of the derived  $v \sin i$  and  $i$  are  $\pm 1$  km/s and  $\pm 5^\circ$ , respectively. These values are between the previous error estimates given by Strassmeier & Rice (2000).

### 3.3 Doppler images of V824 Ara

Doppler surface reconstructions are carried out with the TempMap code originally developed by Rice et al. (1989). The program performs a full LTE spectrum synthesis by solving the equation of transfer through a grid of ATLAS-9 (Kurucz 1993) model atmospheres at all aspect angles and for a given set of chemical abundances. For the synthetic line profiles, the oscillator strengths ( $\log gf$ ) and excitation potentials were taken from the VALD database (Piskunov et al. 1995, Kupka et al. 1999).

For the mapping we select the most commonly used absorption lines with well-known formation physics and mostly free of telluric blends in the vicinity: the Ca I 6439 Å and Fe I 6430 Å lines. We note that in some of the orbital phases at Fe I 6430 Å of the secondary star there is still a

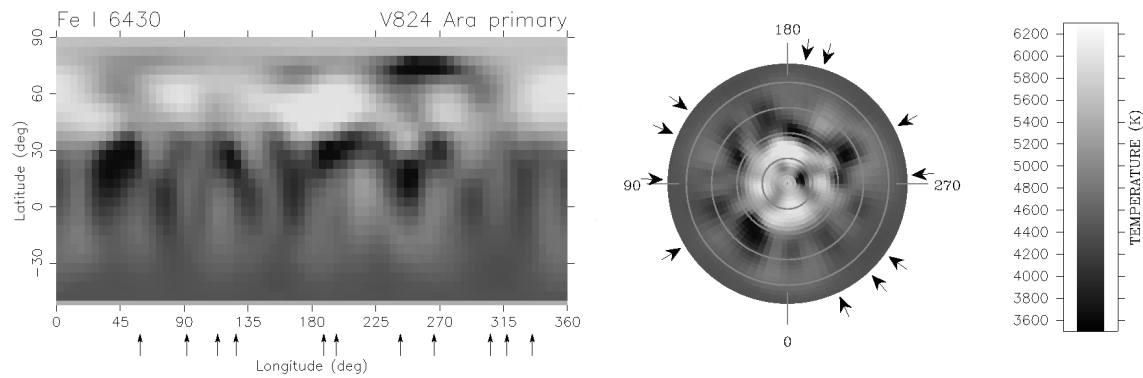


**Fig. 5** Resulting Doppler reconstruction of the primary component of V824 Ara for the Fe I 6430 Å line. The surface temperature map is plotted in pseudo-Mercator projection (left) and in pole-on view (right). Arrows mark the phases of the observations.

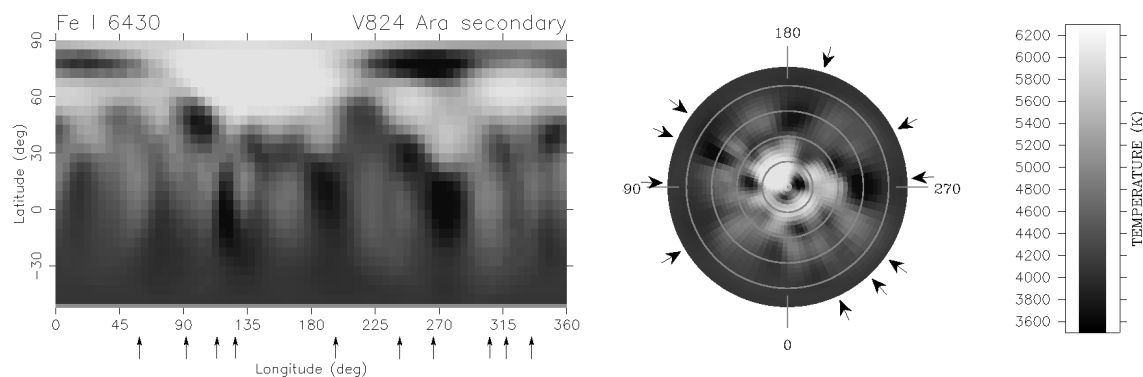


**Fig. 6** Resulting Doppler reconstruction of the secondary component of V824 Ara for the Fe I 6430 Å line. The surface temperature map is plotted in pseudo-Mercator projection (left) and in pole-on view (right). Arrows mark the phases of the observations.

severe blending of the Fe II 6432 Å line which can be eliminated in the iterative process. Resulting Doppler maps for the Ca line are plotted in Fig. 3 (primary comp.) and Fig. 4 (secondary comp.), while Fe line reconstructions are shown in Fig. 5 (primary) and Fig. 6 (secondary). The Ca and Fe line reconstructions reveal similar surface temperature distributions, i.e., mostly cool spots near the poles on both components (more significantly on the the primary star), and sporadic cool spots at lower latitudes. Bright features are also present and are somewhat stronger on the primary component.

#### 4 Summary and discussion

Surface Doppler reconstruction of the components in such a doubly active binary system like our target V824 Ara is still a difficult task because of the overlapping spectra and the larger (twofold) number of astrophysical and atomic parameters. Despite that, we successfully carried out an iterative method which solved the separation of the composite spectra, even when they are disturbed by surface spots. At the end, our step by step method resulted in reliable Doppler reconstructions for both components. The revealed cool spots near the visible poles of both components are in agree-

ment with the previous findings (Hatzes & Kürster 1999, Strassmeier & Rice 2000). On the other hand, low-latitude features seem to be more variable on a longer timescale, as compared to the maps from 1990 (Hatzes & Kürster 1999) and from 1996 (Strassmeier & Rice 2000). Our reconstructions show that bright features appear on the opposing hemispheres. Since these features can be seen on both the Ca I 6439 Å and Fe I 6430 Å maps, we believe that these are indeed real. Strong interactions between the magnetic fields of the members of close RS CVn-type binaries are usual (cf., e.g., Uchida & Sakurai 1985, Siarkowski 1997). We think that the hot spots in our maps (Figs. 3–6) on the components facing each other may indicate such interactions.

*Acknowledgements.* LK, KV, ZsK and OK are grateful to the Hungarian Science Research Program (OTKA) for support under the grant K-81421. This work is supported by the "Lendület-2009" and "Lendület-2012" Young Researchers' Programs of the Hungarian Academy of Sciences and by the HUMAN MB08C 81013 grant of the MAG Zrt.

#### References

- Dunstone, N. J., Hussain, G. A. J., Collier Cameron, A., Marsden, S. C., et al.: 2008, MNRAS 387, 481
- Hatzes, A. P., Kürster, M.:1999, A&A 346, 432

- Kupka, F., Piskunov, N. E., Ryabchikova, T. A., Stempels, H. C., et al.: 1999, *A&AS*, 138, 119
- Kurucz, R. I.: *ATLAS-9*, CD-ROM 13
- Perryman, M. A. C. et al.: 1997, *A&A*, 323, 49
- Piskunov, N. E., Kupka, F., Ryabchikova, T. A., Weiss, W. W., et al.: 1995, *A&AS*, 112, 525
- Piskunov, N., Vincent, A., Duemmler, R., Ilyin, I., et al.: 2001, *ASPC Vol. 223*.
- Rice, J. B., Strassmeier, K. G.: 2000, *A&AS*, 147, 151
- Siarkowski, M. et al.: 1997, *ApJ* 473, 470
- Strassmeier, K. G., Rice, J. B.: 2000, *A&A* 360, 1019
- Strassmeier, K. G., Rice, J. B.: 2003, *A&A* 399, 315
- Uchida, Y., Sakurai, T.: 1985, *IAUS*, 107, 281
- Unruh, Y. C.: 1996, in *Stellar Surface Structure*, ed. K. G. Strassmeier, & J. L. Linsky, *IAU Symp.* 176, 35